Collective magnetic excitations and backbending in fast rotating nuclei

J. Kvasil,[1] N. Lo Iudice,[2] R. G. Nazmitdinov,[3,4] A. Porrino,[2] and F. Knapp[1]
[1]*Institute of Particle and Nuclear Physics, Charles University, V. Holešovičkách 2, CZ-18000 Praha 8, Czech Republic*
[2]*Dipartimento di Scienze Fisiche, Universitá di Napoli "Federico II" and Istituto Nazionale di Fisica Nucleare, Monte S Angelo, Via Cinthia I-80126 Napoli, Italy*
[3]*Departament de Física, Universitat de les Illes Balears, E-07122 Palma de Mallorca, Spain*
[4]*Bogoliubov Laboratory of Theoretical Physics, Joint Institute for Nuclear Research, 141980 Dubna, Russia*
(Received 9 March 2004; published 7 June 2004)

We study in cranked Nilsson plus random phase approximation the electric monopole ($E0$), quadrupole ($E2$), and magnetic dipole ($M1$) responses in fast rotating nuclei undergoing backbending, more specifically ^{156}Dy and ^{158}Er. Special attention is paid at the orbital $M1$ excitations known as scissors mode. We find that the overall strength of the orbital $M1$ transitions gets enhanced by more than a factor of 4 above the critical backbending region. We show that such a strength evolves with the rotational frequency in close correspondence with the nuclear moment of inertia. This link provides the main clue for understanding the physical origin of such an enhancement, which, if experimentally confirmed, would represent a distinctive feature of nuclei exhibiting backbending.

DOI: 10.1103/PhysRevC.69.064308 PACS number(s): 21.10.Re, 21.60.Jz, 27.70.+q

I. INTRODUCTION

Deformation is known to affect deeply the collective nuclear motion [1]. It is responsible for the splitting of the electric giant dipole [2,3], quadrupole [4], and octupole [5,6] resonances, as well as for the coupling between quadrupole and monopole collective modes [7–9]. Deformation generates also new magnetic dipole excitations of orbital nature, known as scissors mode [10–12].

Thanks to heavy-ion accelerators and a new generation of detectors, it was possible to get access to fast rotating nuclei and to observe quite new phenomena induced by rapid rotation. Backbending is a well-known spectacular example [13]. Systematic theoretical investigations have clarified to a great extent how fast rotation affects most of the nuclear properties, including β and γ modes [14,15], low-lying octupole excitations and alignment [16–18], and pairing vibrations [19,20]. All these studies were carried out in cranked random phase approximation (CRPA) using separable effective interactions. The same approach was adopted for extensive studies of the electric giant dipole resonance [21,22].

Less explored is the effect of rotation on other collective excitations. To our knowledge, monopole and quadrupole resonances were studied only in Ref. [23] within the CRPA, using the cranked modified harmonic oscillator (HO), and in Ref. [9] within a phonon-plus-rotor model, using schematic RPA to generate the phonons.

In the present paper, we intend to complete the analysis of Refs. [9,23] by including a study of the $M1$ excitations, with special attention at those of orbital nature generating the scissors mode. Such a mode is tightly linked to deformation and, more in general, to quadrupole correlations. Moreover, by its own nature, it is strongly correlated with nuclear rotation. Its properties might therefore change considerably with increasing angular frequencies, especially in nuclei whose inertial parameters are strongly affected by fast rotation. Thus, nuclei undergoing backbending are expected to display more clearly the effects of rotation on the magnetic excitations.

Our approach is framed within the CRPA and parallels closely the model of Ref. [18]. We adopt, in fact, a cranked Nilsson plus quasiparticle RPA using a two-body potential of separable form. Its multipole pieces are expressed in terms of doubly stretched coordinates so as to restore the rotational symmetry broken by the rotating one-body field. There are, nevertheless, several differences with respect to the approach of Ref. [18]. They concern mainly the choice and treatment of the Hamiltonian as well as the method for computing the electromagnetic response.

We apply our procedure to two typical nuclei exhibiting backbending, ^{156}Dy and ^{158}Er. The evolution of their moment of inertia with the rotational frequency was studied within an approach using the same mean field adopted here and found to be consistent with the behavior observed experimentally, including the backbending region [24]. This strengthens our confidence on the reliability of our predictions on the $M1$ mode, whose properties, as we shall see, depend critically on the nuclear moment of inertia.

II. RPA IN THE ROTATING FRAME

A. The Hamiltonian

We start with the Hamiltonian,

$$H_\Omega = H - \hbar\Omega\hat{I}_1 = H_0 - \sum_{\tau=n,p} \lambda_\tau N_\tau - \hbar\Omega I_1 + V. \qquad (1)$$

The unperturbed term consists of two pieces,

$$H_0 = \sum_i (h_{\rm Nil}(i) + h_{\rm add}(i)). \qquad (2)$$

The first is the Nilsson Hamiltonian

$$h_{\rm Nil} = \frac{p^2}{2m} + V_{\rm HO} + v_{ls}\mathbf{l}\cdot\mathbf{s} + v_{ll}(\mathbf{l}^2 - \langle\mathbf{l}^2\rangle_N), \qquad (3)$$

where

$$V_{\rm HO} = \tfrac{1}{2}m(\omega_1^2 x_1^2 + \omega_2^2 x_2^2 + \omega_3^2 x_3^2) \tag{4}$$

is a triaxial HO potential, whose frequencies satisfy the volume conserving condition $\omega_1\omega_2\omega_3 = \omega_0^3$. The second piece of H_0 restores the local Galilean invariance broken in the rotating coordinate system and has the form [18]

$$h_{\rm add} = -\frac{\Omega}{\sqrt{\omega_2\omega_3}}\left\{ \upsilon_{ll}\left[2m\omega_0 \mathbf{r}'^2 - \hbar\left(N_{\rm osc} + \frac{3}{2}\right)\right] l_1' + \upsilon_{ls} m\omega_0 [\mathbf{r}'^2 \mathbf{s_1} - \mathbf{x_1'}(\mathbf{r}' \cdot \mathbf{s})]\right\}, \tag{5}$$

where $x_i' = (\omega_i/\omega_0)^{1/2} x_i$ are single-stretched coordinates.

The two-body potential has the following structure:

$$V = V_{PP} + V_{QQ} + V_{MM} + W_{\sigma\sigma}. \tag{6}$$

V_{PP} is a monopole pairing,

$$V_{PP} = -\sum_{\tau=p,n} G_\tau P_\tau^\dagger P_\tau, \tag{7}$$

where $P_\tau^\dagger = \Sigma_k\, a_k^\dagger a_{\bar{k}}^\dagger$. V_{QQ} and V_{MM} are, respectively, separable quadrupole–quadrupole and monopole–monopole potentials,

$$V_{QQ} = -\frac{1}{2}\sum_{T=0,1} \kappa(T) \sum_{r=\pm}\sum_{\mu=0,1,2} \left(\tilde{Q}_\mu \begin{bmatrix} T \\ r \end{bmatrix}\right)^2,$$
$$V_{MM} = -\frac{1}{2}\sum_{T=0,1} \kappa(T) \left(\tilde{M} \begin{bmatrix} T \\ r = + \end{bmatrix}\right)^2. \tag{8}$$

$V_{\sigma\sigma}$ is a spin–spin interaction

$$V_{\sigma\sigma} = -\frac{1}{2}\sum_{T=0,1} \kappa_\sigma(T) \sum_{r=\pm}\sum_{\mu=0,1} \left(s_\mu \begin{bmatrix} T \\ r \end{bmatrix}\right)^2. \tag{9}$$

Because of its repulsive character, this interaction pushes the spin excitations at higher energies, in the range 4 MeV–12 MeV, well separated from the region of the orbital excitations below 4 MeV [25,26].

All the one-body fields have good isospin T and signature r. Multipole and spin-multipole fields of good signature are defined in Ref. [27]. The tilde indicates that monopole and quadrupole fields are expressed in terms of doubly stretched coordinates $x_i'' = (\omega_i/\omega_0)x_i$ [4,28]. In this new form, for a pure HO Hamiltonian, the quadrupole fields fulfill the stability conditions

$$\langle \tilde{Q}_\mu \rangle = 0, \quad \mu = 0,1,2 \tag{10}$$

if nuclear self-consistency

$$\omega_1^2\langle x_1^2\rangle = \omega_2^2\langle x_2^2\rangle = \omega_3^2\langle x_3^2\rangle \tag{11}$$

is satisfied in addition to the volume conserving constraint. In virtue of the stability conditions (10), the interaction will not distort further the deformed HO potential, if the latter is generated as a Hartree field. To this purpose, one starts with an isotropic HO potential of frequency ω_0 and, then, generates the deformed part of the potential from the (unstretched) quadrupole–quadrupole interaction. The outcome of this procedure is

$$V_{\rm HO} = \frac{m\omega_0^2 r^2}{2} - m\omega_0^2\beta\cos\gamma Q_0\begin{bmatrix} 0 \\ + \end{bmatrix} - m\omega_0^2\beta\sin\gamma Q_2\begin{bmatrix} 0 \\ + \end{bmatrix}, \tag{12}$$

where

$$m\omega_0^2\beta\cos\gamma = \kappa[0]\left\langle Q_0\begin{bmatrix} 0 \\ + \end{bmatrix}\right\rangle,$$
$$m\omega_0^2\beta\sin\gamma = \kappa[0]\left\langle Q_2\begin{bmatrix} 0 \\ + \end{bmatrix}\right\rangle. \tag{13}$$

The triaxial form given by Eq. (4) follows from defining

$$\omega_i = \omega_0 \exp\left[-\frac{2}{3}\delta\cos\left(\gamma - i\frac{2\pi}{3}\right)\right], \quad i = 1,2,3, \tag{14}$$

where the new deformation parameter is defined by $\beta = \sqrt{16\pi/45}\,\delta$. The Hartree conditions have the form given by Eq. (13) only for a HO potential plus a separable quadrupole–quadrupole interaction. They change if pairing is added [29] and, moreover, fail to yield a minimum for the mean field energy of the rotating system in superdeformed nuclei [30]. Due to all these facts, we allow small deviations from Eqs. (13) and enforce only the stability conditions (10). These, in fact, hold also in the presence of pairing [24] and ensure the separation of the pure rotational mode from the intrinsic excitations for a cranked harmonic oscillator [31].

B. Quasiparticle RPA in rotating systems

By means of a generalized Bogoliubov transformation, we express the Hamiltonian given by Eq. (1) in terms of quasiparticle creation ($\alpha_i^\dagger$) and annihilation (α_i) operators. We then face the RPA equations of motion, written in the form [14,27]

$$[H_\Omega, P_\nu] = i\hbar\omega_\nu^2 X_\nu, \quad [H_\Omega, X_\nu] = -i\hbar P_\nu, \quad [X_\nu, P_{\nu'}] = i\hbar\delta_{\nu\nu'}, \tag{15}$$

where X_ν, P_ν are, respectively, the collective coordinates and their conjugate momenta. The solution of the above equations yields the RPA eigenvalues $\hbar\omega_\nu$ and eigenfunctions

$$|\nu\rangle = O_\nu^\dagger|\mathrm{RPA}\rangle = \frac{1}{\sqrt{2}}\left(\sqrt{\frac{\omega_\nu}{\hbar}} X_\nu - \frac{i}{\sqrt{\hbar\omega_\nu}}\hat{P}_\nu\right)|\mathrm{RPA}\rangle$$
$$= \sum_{ij} (\psi_{ij}^\nu b_{ij}^\dagger - \Phi_{ij}^\nu b_{ij})|\mathrm{RPA}\rangle, \tag{16}$$

where $b_{ij}^\dagger = \alpha_i^\dagger\alpha_j^\dagger (b_{ij} = \alpha_i\alpha_j)$ creates (destroys) a pair of quasiparticles out of the RPA vacuum $|\mathrm{RPA}\rangle$. Since the Hamiltonian can be decomposed into the sum of a positive and a negative signature terms

$$H_\Omega = H_\Omega(r = +) + H_\Omega(r = -), \tag{17}$$

we solve the eigenvalue equations (15) for $H_\Omega(+)$ and $H_\Omega(-)$, separately.

The symmetry properties of the cranking Hamiltonian yield

$$[H,N_{\tau=n,p}]_{\mathrm{RPA}}=0, \quad [H,I_1]_{\mathrm{RPA}}=0, \tag{18}$$

$$[H,I_2]_{\mathrm{RPA}}=i\hbar\Omega I_3, \quad [H,I_3]_{\mathrm{RPA}}=-i\hbar\Omega I_2. \tag{19}$$

The last two equations can be combined so as to obtain

$$[H_\Omega(-),\Gamma^\dagger]=\Omega\Gamma^\dagger, \tag{20}$$

where $\Gamma^\dagger=(I_2+iI_3)/\sqrt{2\langle I_1\rangle}$ and $\Gamma=(\Gamma^\dagger)^\dagger=(I_2-iI_3)/\sqrt{2\langle I_1\rangle}$ fulfill the commutation relation

$$[\Gamma,\Gamma^\dagger]=1. \tag{21}$$

According to Eqs. (18), we have two Goldstone modes, one associated with the violation of the particle number operator, the other is a positive signature zero frequency rotational solution associated with the breaking of spherical symmetry. Equation (20), on the other hand, yields a negative signature redundant solution of energy $\omega_\lambda=\Omega$, which describes a collective rotational mode arising from the symmetries broken by the external rotational field (the cranking term).

Equations (18) and (20) ensure the separation of the spurious or redundant solutions from the intrinsic ones. They would be automatically satisfied if the single-particle basis were generated by means of a self-consistent Hartree–Bogoliubov (HB) calculation. As we shall show, they are fulfilled with a good accuracy also in our, not fully self-consistent, HB treatment.

The strength function for an electric ($X=E$) or magnetic ($X=M$) transition of multipolarity λ from a state of the yrast line with angular momentum I is

$$S_{X\lambda}(E)=\sum_{\nu I'} B(X\lambda, I\rightarrow I',\nu)\,\delta(E-\hbar\omega_\nu), \tag{22}$$

where ν labels all the excited states with a given I'. In order to compute the reduced strength $B(X\lambda, I\rightarrow I',\nu)$ we should be able to expand the intrinsic RPA state into components with good K quantum numbers, which is practically impossible in the cranking approach. We compute, therefore, the strength in the limits of zero and high angular frequencies. For nonrotating axially symmetric nuclei, whose initial state is usually the $I=0, K^\pi=0^+_{\mathrm{gr}}$ ground state, the strength function is given by

$$S_{X\lambda}(E)=\sum_{\nu K} B(X\lambda, 0^+_{\mathrm{gr}}\rightarrow K\nu)\,\delta(E-\hbar\omega_\nu), \tag{23}$$

where

$$B(X\lambda, 0^+_{\mathrm{gr}}\rightarrow K_\nu)=|\langle \mathrm{RPA}|[O_{K\nu},\mathcal{M}(X\lambda\mu_3=K)]|\mathrm{RPA}\rangle|^2. \tag{24}$$

For fast rotating nuclei, we assume a complete alignment of the angular momentum along the rotational x_1 axis, so that ($I'=I+\Delta I$)

$$S_{X\lambda,\Omega(I)}(E)=\sum_{\nu\Delta I} B(X\lambda, I\ yrast\rightarrow I+\Delta I,\nu r)\,\delta(E-\hbar\omega_\nu), \tag{25}$$

where ($\Delta I=0,\pm1,\ldots,\pm\lambda$)

$$B(X\lambda, I\rightarrow I+\Delta I,\nu r)=|(I\ I\lambda\Delta I|I+\Delta I\ I+\Delta I)_\Omega \times\langle \mathrm{RPA}|[O_{\nu r},\mathcal{M}(X\lambda\mu_1=\Delta I)]|\mathrm{RPA}\rangle_\Omega|^2. \tag{26}$$

Here, $|\mathrm{RPA}\rangle_\Omega$ denotes the RPA vacuum (*yrast* state) at the rotational frequency Ω. The multipole operator in the rotating frame is obtained from the corresponding one in the laboratory according to the prescription [32]

$$\mathcal{M}(X\lambda\mu_1)=\sum_{\mu_3}\mathcal{D}^\lambda_{\mu_1\mu_3}\left(0,\frac{\pi}{2},0\right)\mathcal{M}(X\lambda\mu_3). \tag{27}$$

The strength function method allows to avoid the explicit determination of RPA eigenvalues and eigenfunctions [14,27]. We just have to replace the δ distribution with a Lorentz weight. Thus, upon the use of the Cauchy theorem, we obtain for $S_{X\lambda}(E)$ and $S_{X\lambda,\Omega(I)}(E)$ expressions involving only two quasiparticle matrix elements of one-body multipole operators.

The nth moments are obtained simply as

$$m_n(X\lambda)=\int_0^\infty E^n S_{X\lambda}(E)\,dE. \tag{28}$$

The $m_0(X\lambda)$ and $m_1(X\lambda)$ moments give, respectively, the energy unweighted and weighted summed strengths.

III. NUMERICAL CALCULATIONS AND RESULTS

A. Determination of the parameters

The parameters of the Nilsson potential were taken from Ref. [33]. They were determined from a systematic analysis of the experimental single-particle levels of deformed nuclei of rare earth and actinide regions. In our calculation, we included all shells up to $N=8$ and accounted for the $\Delta N=2$ mixing.

In principle, the pairing gap should be determined self-consistently at each rotational frequency. In order to avoid unwanted singularities for certain values of Ω, we followed the phenomenological prescription [34]:

$$\Delta_\tau(\Omega)=\begin{cases}\Delta_\tau(0)\left[1-\frac{1}{2}\left(\frac{\Omega}{\Omega_c}\right)^2\right], & \Omega<\Omega_c,\\ \Delta_\tau(0)\frac{1}{2}\left(\frac{\Omega_c}{\Omega}\right)^2, & \Omega>\Omega_c,\end{cases} \tag{29}$$

where Ω_c is the critical rotational frequency of the first band crossing. We obtained, for both neutrons and protons, $\Omega_c=0.32$ MeV for ^{156}Dy and $\Omega_c=0.33$ MeV for ^{158}Er. The values of the pairing gaps at zero rotational frequency were deduced from the odd–even mass differences, obtaining $\Delta_N(0)=0.857$ MeV, $\Delta_P(0)=0.879$ MeV for ^{156}Dy and $\Delta_N(0)=0.874$ MeV, $\Delta_P(0)=0.884$ MeV for ^{158}Er.

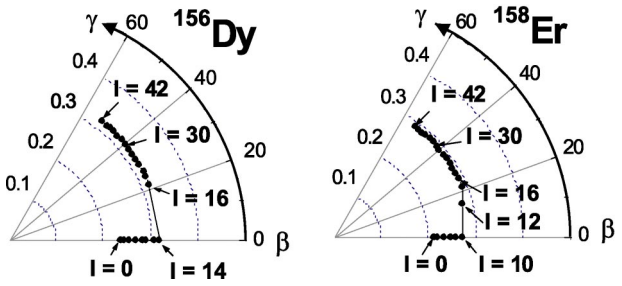

FIG. 1. (Color online) Equilibrium deformations in $\beta-\gamma$ plane as a function of the angular momentum.

We used as input for our HB calculations the deformation parameters obtained from the empirical moments of inertia at each Ω [35]. As shown in Fig. 1 and discussed elsewhere [24], triaxiality sets in at the frequency which triggers backbending as a result of the vanishing of the gamma excitations of positive signature in the rotating frame.

The parameters so determined yield results in better agreement with experiments, compared to the ones obtained in Ref. [36] for $N\sim 90$, where fixed phenomenological inertial parameters were used for all Ω frequencies. Moreover, our equilibrium deformations are short from being the self-consistent solutions of the HB equations. Indeed, any deviation from the equilibrium values of the deformation parameters β and γ results into a higher HB energy. Dealing with transitional nuclei, however, the minimum becomes very shallow as the rotational frequency increases. In fact, the energy minima for the collective rotation around the x_1 rotational axis and for the noncollective one around the x_3 symmetry axis are almost degenerate near the crossing point of the ground with the gamma band. The energy difference is about 15 keV near the critical rotational frequency where the backbending occurs. At the bifurcation point, the competition between collective and noncollective rotations breaks the axial symmetry and yields nonaxial shapes. On the other hand, the doubly stretched quadrupole moments are approximately zero for all values of the equilibrium deformation parameters, consistently with the stability conditions (10). A small deviation from the equilibrium deformation yields a strong deviation of these moments from zero. We infer from the just discussed tests that our solutions are close to the self-consistent HB ones.

In order to determine the strength κ of the monopole and quadrupole interactions, we used the standard HO formulas ($\lambda=2$) [28]

$$\kappa_\lambda[0]=\frac{4\pi}{2\lambda+1}\frac{m\omega_0^2}{A\langle r^{2\lambda-2}\rangle},\quad \kappa_\lambda[1]=-\frac{\pi V_1}{A\langle r^{2\lambda}\rangle}. \qquad (30)$$

For instance, the isoscalar strength follows from enforcing the Hartree self-consistent conditions. We then changed slightly the strengths at each rotational frequency, while keeping constant the $\kappa[1]/\kappa[0]$ ratio, so as to fulfill the RPA equations (18)–(20) for the spurious or redundant modes. The constants so determined differ from the HO ones by 5–10 % at most. For the spin–spin interaction, we used the generally accepted strengths [37]

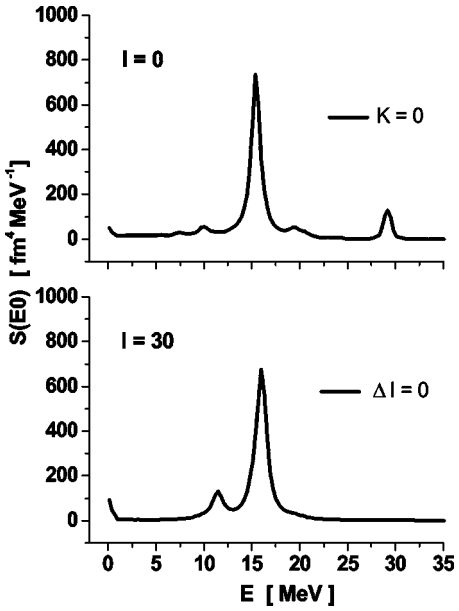

FIG. 2. $E0$ strength function at zero and high rotational frequencies in ^{156}Dy.

$$\kappa_\sigma[0]=\kappa_\sigma[1]=-28\frac{4\pi}{A}\text{MeV}$$

for all rotational frequencies. Finally, we adopted bare charges to compute the $E0$ and $E2$ strengths and a quenching factor $g_s=0.7$ for the spin gyromagnetic ratios to compute the $M1$ strengths.

By using the above set of parameters, it was possible not only to separate the spurious and rotational solutions from the intrinsic modes, but also to reproduce the experimental dependence of the lowest β and γ bands on Ω and, in particular, to observe the crossing of the γ with the ground band in correspondence with the onset of triaxiality [24].

B. Evolution of transition strengths with rotational frequency

We show the results of ^{156}Dy only, since the ones pertaining to ^{158}Er are very similar. As shown in Fig. 2, the $E0$ response remains unchanged in its dominant isoscalar peak. The effects of fast rotation get manifest via the suppression of the high energy isovector peak, small in any case, and the appearance of a peak at $\sim$11–12 MeV, in correspondence with the $K=0$ branch of the quadrupole resonance. This result indicates that the coupling between monopole and $K=0$ quadrupole modes gets stronger as the rotational frequency increases. Indeed, as triaxiality sets in at high frequencies, the anisotropy increases, thereby enhancing the mixing between the two channels.

Fast rotation has some appreciable effects on the quadrupole transitions. It broadens considerably the isoscalar quadrupole giant resonance due to the increasing splitting of the different ΔI peaks with increasing Ω. It washes out the isovector $E2$ resonance for the same reason. The low-lying peaks shown in Fig. 3 are related to γ, β excitations and to the collective rotational modes described by Eq. (20). Since these low-lying excitations have been discussed elsewhere

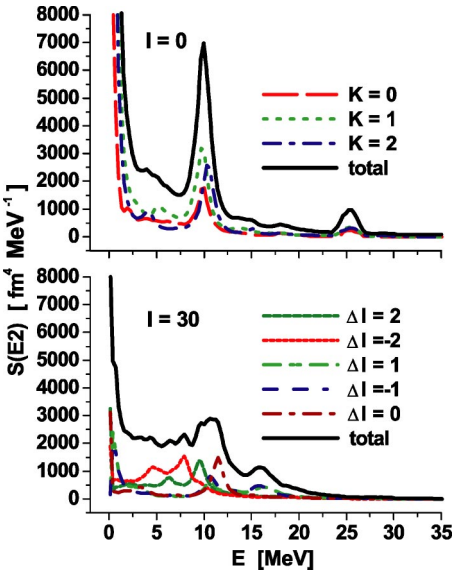

FIG. 3. (Color online) $E2$ strength function at zero and high rotational frequencies in ^{156}Dy.

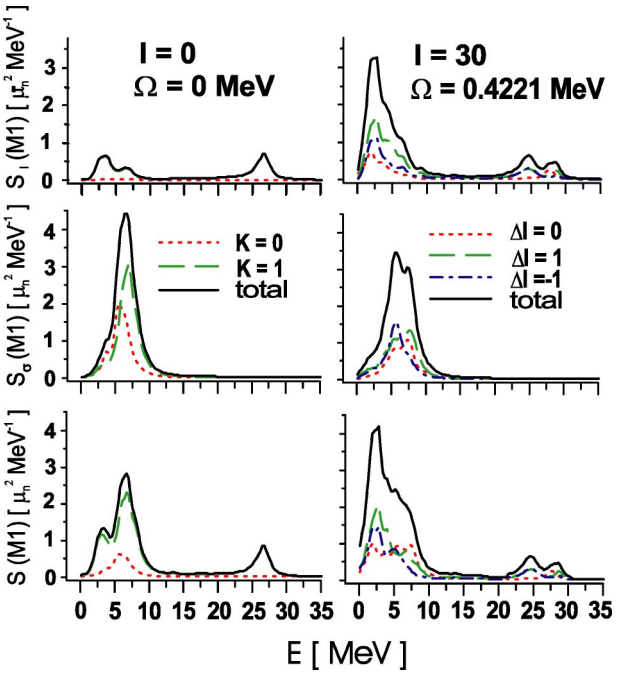

FIG. 4. (Color online) Orbital, spin, and total $M1$ strength functions at zero (left-hand panels) and high rotational frequencies (right-hand panels) in ^{156}Dy.

[24], we will focus our study upon the excitations located at higher energies.

The moment $m_1(E2)$ exhausts more than 98% of the oscillator $E2$ energy-weighted sum rule (EWSR)

$$m_1(E2) = \frac{15}{2\pi}\frac{\hbar^2}{2m}AR_0^2$$

for all values of Ω. The same result holds for the $E0$ mode. Thus, the $E0$ and $E2$ EWSR are not affected by rotation.

At zero rotational frequency, the strength of the magnetic dipole transitions is concentrated in three distinct regions, consistently with the theoretical expectations and the experimental findings [12]. The low-energy interval, ranging from 2 to 4 MeV, is characterized by orbital excitations (scissors mode [10,11]). The high-energy one, located around 24 MeV, consists also of orbital excitations (high energy scissors mode [38]). The intermediate region, ranging from 4 to 12 MeV, is due to spin excitations [39].

As shown in Fig. 4, the distribution of the strength changes considerably as Ω increases, to the point that the dominant peak shifts from 7–8 MeV down to 3 MeV. Only in the high energy region, the changes, though appreciable, are not dramatic. Here, the $M1$ strength gets more spread and increases slightly in magnitude (Table I).

For a deeper insight, we analyze separately the contribution of orbital and spin excitations up to 10 MeV. As shown in Fig. 5, the rotation broadens the spin strength at the expenses of the main peaks which get severely reduced. The fragmentation keeps the spin transitions confined mainly within the range 4–12 MeV (Table I).

The low-lying orbital strength becomes larger and larger as Ω increases. At $\Omega=0$, the orbital peaks are small compared to the spin transitions which are dominant in the $M1$ spectrum. At $I=30\hbar$, instead, the orbital spectrum covers a wider energy range. Furthermore, it gets magnified, especially in the low-energy sector, where we obtain quite high peaks. The low-lying orbital strength increases by more than a factor of 6 due to fast rotation (Table I). One may also observe that the $\Delta I=0$ transitions, absent at zero frequency ($\Delta I=K=0$), give a small but nonzero contribution which increases with Ω. This is due to a new branch of the scissors mode which arises with the onset of triaxiality [40,41]. Indeed, in the transition from the axial to the triaxial shape, the mode splits into two branches of energy and $M1$ strength

$$E_i = \cos\ \gamma\left[1-(-1)^i\frac{1}{\sqrt{3}}\tan\ \gamma\right]E_{\rm sc},$$
$$B_i(M1) = \frac{1}{2}\cos\ \gamma\left[1-(-1)^i\frac{1}{\sqrt{3}}\tan\ \gamma\right]B_{\rm sc}(M1), \quad i=1,2 \tag{31}$$

where $E_{\rm sc}$ and $B_{\rm sc}(M1)$ are the energy and the strength in the axial case. These two branches describe the rotational oscillations around the x_1 and x_2 axes. A new $K=0$ branch also arises due to the rotational oscillation around the x_3 axis. Its energy and strength are given by

$$E_3 = \frac{2}{\sqrt{3}}\sin\ \gamma E_{\rm sc},$$
$$B_3(M1)\uparrow = \frac{2}{\sqrt{3}}\sin\ \gamma B_{\rm sc}(M1). \tag{32}$$

The increasing role of the orbital motion with the increase of the rotational frequency can be also inferred from the plot of the running sums shown in Fig. 6.

TABLE I. Orbital, spin, and total $M1$ strengths integrated over different energy ranges at zero and high ($\Omega = 0.4221$ MeV) rotational frequencies.

	1 MeV $< E <$ 4 MeV		4 MeV $< E <$ 12 MeV		$E >$ 12 MeV	
	$I=0$	$I=30$	$I=0$	$I=30$	$I=0$	$I=30$
$\Sigma B_l(M1)[\mu_n^2]$	1.36	8.87	1.43	5.39	2.75	4.35
$\Sigma B_\sigma(M1)[\mu_n^2]$	1.92	3.08	14.97	14.47	0.48	0.68
$\Sigma B(M1)[\mu_n^2]$	2.95	12.21	9.82	10.06	3.57	4.58

The orbital strength, small at zero frequency in the whole energy range, becomes by far larger than the spin strength in the low-energy sector at high frequencies.

We can identify one of the mechanisms responsible for such a large enhancement by comparing (Fig. 7) the Ω behavior of the orbital and total $m_1(M1)$ moments with the corresponding evolution of the kinematical moment of inertia $\Im = I/\Omega$, computed using the cranking method of Ref. [30].

The strikingly similar behavior of the orbital $m_1(M1)$ and the moment of inertia shows that the two quantities are closely correlated at all rotational frequencies. Indeed, at zero frequency, one has the $M1$ EWSR [42,43],

$$m_1^{(\mathrm{sc})}(M1) = \sum_n E_n B_n^{(\mathrm{sc})}(M1) \simeq \frac{9}{16\pi}(\kappa(0) - \kappa(1))\langle Q(0)\rangle^2, \tag{33}$$

where $Q(0) = Q_p + Q_n$ is the isoscalar quadrupole field. Using the HO formulas (30) for the coupling constants and the standard expression for the quadrupole moment [1], we get for the right-hand side

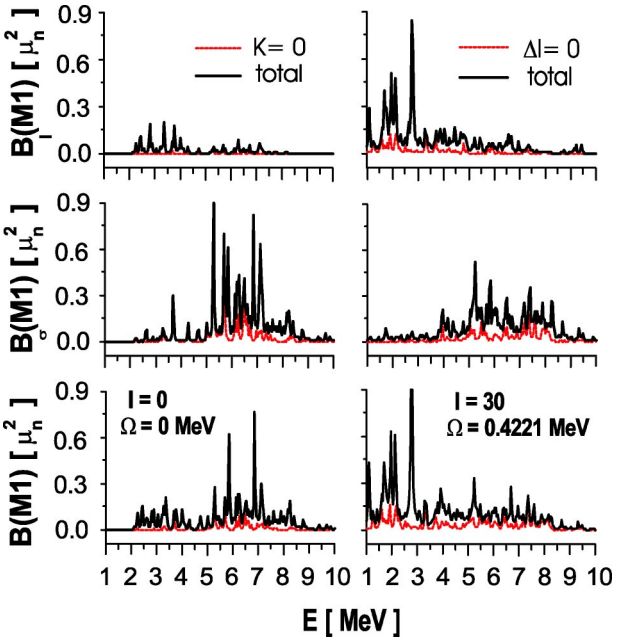

FIG. 5. (Color online) Orbital, spin, and total $M1$ reduced strength distributions at zero (left-hand panels) and high rotational frequencies (right-hand panels) in ^{156}Dy.

$$m_1^{(\mathrm{sc})}(M1) = \frac{3}{8\pi}(1-b)\Im_{\mathrm{rig}}\omega_0^2\delta^2, \tag{34}$$

where $b = \kappa(1)/\kappa(0)$ and

$$\Im_{\mathrm{rig}} = \tfrac{2}{3}mA\langle r^2\rangle. \tag{35}$$

This expression shows explicitly the close link between the orbital $M1$ EWSR and the moment of inertia, at zero rotational frequency. We get a deeper insight by inspecting more closely the energy unweighted and weighted sums. For both low- and high-energy modes, the $M1$ summed strength has the general form [12]

$$m_0^{(\pm)}(M1) = \sum_{n_\pm} B_{n_\pm}^{(\pm)}(M1) \simeq \frac{3}{16\pi}\Im_{\mathrm{sc}}^{(\pm)}\overline{E}^{(\pm)}, \tag{36}$$

where $\overline{E}^{(\pm)}$ and $\Im_{\mathrm{sc}}^{(\pm)}$ denote the energy centroids and the mass parameters of the high-lying (+) and low-lying (−) scissors modes.

At high energy, protons and neutrons behave as normal irrotational fluids, so that energy and mass parameter are given by

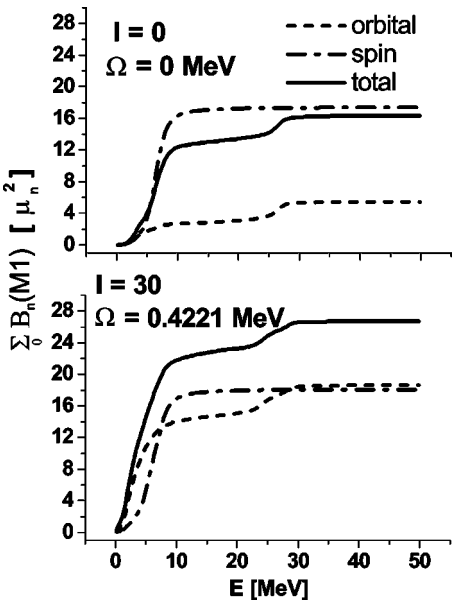

FIG. 6. Running sum of the orbital (dashed line), spin (dashed–dotted line), and total (solid line) $M1$ strength in ^{156}Dy.

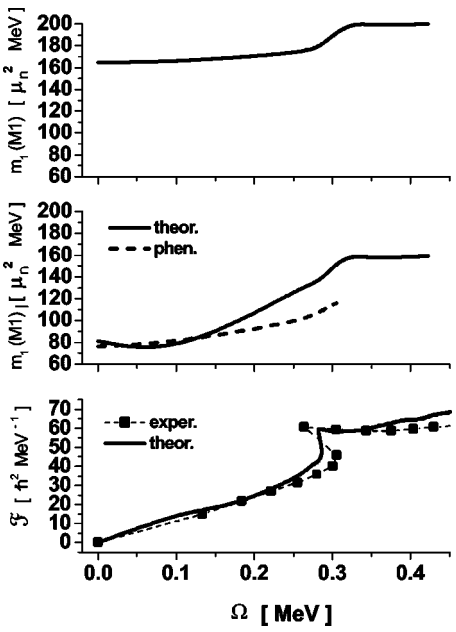

FIG. 7. Total (top panel), orbital (middle panel) $m_1(M1)$ moments and the kinematical moment of inertia (bottom panel) versus Ω in ^{156}Dy. The dashed line in the middle panel displays the $M1$ EWSR at zero frequency computed from Eq. (33) (taken from Ref. [43]).

$$\overline{E^{(+)}} \propto 2\omega_0, \quad \mathfrak{I}_{\rm sc}^{(+)} = \mathfrak{I}_{\rm irr} = \mathfrak{I}_{\rm rig}\delta^2, \tag{37}$$

and, therefore, yield

$$m_0^{(+)}(M1) = \sum_{n_+} B_{n_+}^{(+)}(M1) \propto \mathfrak{I}_{\rm rig}\delta^2,$$
$$m_1^{(+)}(M1) \simeq \overline{E^{(+)}} \sum_{n_+} B_{n_+}^{(+)} \propto \mathfrak{I}_{\rm rig}\delta^2. \tag{38}$$

Thus, both $M1$ weighted and unweighted summed strengths are quadratic in the deformation parameter. This result remains substantially unchanged in fast rotating nuclei.

For the low-energy mode, instead, we must distinguish between zero and high rotational frequencies. At zero frequency, protons and neutrons behave as superfluids, so that [44,45]

$$\overline{E^{(-)}} \propto 2E_{\rm qp} \simeq 2\Delta, \quad \mathfrak{I}_{\rm sc}^{(-)} = \mathfrak{I}_{\rm sf} \propto \mathfrak{I}_{\rm rig}\delta^2, \tag{39}$$

where $E_{\rm qp}$ denotes the quasiparticle energy and $\mathfrak{I}_{\rm sf}$ the superfluid moment of inertia. We then have

$$m_0^{(-)}(M1) = \sum_{n_-} B_{n_-}^{(-)}(M1) \propto \mathfrak{I}_{\rm rig}\delta^2,$$
$$m_1^{(-)}(M1) \simeq \overline{E^{(-)}} \sum_{n_-} B_{n_-}^{(-)}(M1) \propto \mathfrak{I}_{\rm rig}\delta^2. \tag{40}$$

These relations show that $m_1(M1)$ is consistent with the EWSR (33) and, quite remarkably, the summed strength $m_0(M1)$ follows the quadratic deformation law found experimentally [46,47].

At high rotational frequency, instead, the pairing correlations are quenched, so that protons and neutrons behave basically as rigid rotors. We have therefore

$$\overline{E^{(-)}} \propto \delta\omega_0, \quad \mathfrak{I}_{\rm sc}^{(-)} \simeq \mathfrak{I}_{\rm rig}. \tag{41}$$

These yield

$$m_0^{(-)}(M1) = \sum_{n_-} B_{n_-}^{(-)} \propto \mathfrak{I}_{\rm rig}\delta,$$
$$m_1^{(-)}(M1) \simeq \overline{E^{(-)}} \sum_{n_-} B_{n_-}^{(-)} \propto \mathfrak{I}_{\rm rig}\delta^2. \tag{42}$$

According to the above formulas, the superfluid to normal phase transition affects the deformation law. While, in fact, the energy-weighted sum remains quadratic in the deformation, the behavior of the unweighted summed strength with δ changes from quadratic to linear.

We, therefore, conclude that the scissors $M1$ strength is closely correlated with the nuclear moment of inertia not only at low but also at high angular frequencies. More specifically, we can distinguish two different regimes, one below the backbending critical frequency and the other above. Below backbending, while the quasiparticle energy moves downward due to the weakening of pairing, the $M1$ strength increases with Ω due to the increasing axial deformation and the smooth enhancement of the moment of inertia. Above the backbending critical value, when the nucleus undergoes a transition from a superfluid to an almost rigid phase, as a result of the alignment of few quasiparticles with high angular momenta, the $M1$ strength jumps to a plateau, due to a sudden increase of the moment of inertia, while the deformation parameter δ remains practically constant.

Also the onset of triaxiality raises $m_1(M1)$ at high rotational frequency, to a modest extent. Indeed, from Eqs. (31) and (32) we get $(i=1,2,3)$

$$\sum_i E_i^{(-)} B_i^{(-)}(M1) \uparrow = \left(1 + \frac{5}{18}\sin^2\gamma\right) m_1^{(-)}(M1). \tag{43}$$

For $\gamma = 50^0$, $m_1^{(-)}(M1)$ increases by a factor of 1.16. A further contribution comes from the changes in the shell structure induced by fast rotation. This, indeed, enhances the number of configurations taking part to the motion over the whole energy range. The new configurations generate new transitions on the one hand, and, on the other hand, enhance the amplitudes of collective as well as noncollective transitions.

IV. CONCLUSIONS

Our analysis shows that fast rotation strengthens the coupling between quadrupole and monopole modes, broadens appreciably the isoscalar quadrupole giant resonance and washes out the isovector monopole and quadrupole peaks. These effects are found to be more appreciable than the ones predicted in Ref. [23]. On the other hand, the two approaches differ in several details. We accounted for the $\Delta N=2$ coupling in generating the Nilsson states and included the Galilean invariance restoring piece according to the prescription

of Ref. [18]. Moreover, we enforced the HB stability conditions, provided by Eq. (10), that yield deformation parameters very close to the self-consistent values. Finally, we fixed the strength parameters of the interaction so as to ensure the separation of the spurious modes from the intrinsic excitations at each rotational frequency.

The most meaningful and intriguing result of our calculation concerns the orbital, scissors-like, $M1$ excitations. The enhancement of the overall $M1$ strength at high rotational frequencies emphasizes the dominant role of the scissors mode over spin excitations in fast rotating nuclei and represents an additional signature for superfluid to normal phase transitions in deformed nuclei. If confirmed experimentally, this feature would provide new information on the collective properties of deformed nuclei.

ACKNOWLEDGMENTS

This work was partly supported by the Czech grant agency under Contract No. 202/02/0939, the Italian Ministero dell'Istruzione, Universitá and Ricerca (MIUR) and by Grant No. BFM2002-03241 from DGI (Spain). R.G.N. gratefully acknowledges support from the Ramón y Cajal program (Spain).

[1] A. Bohr and B. R. Mottelson, *Nuclear Structure* (Benjamin, New York, 1975), Vol. II.
[2] M. Danos, Nucl. Phys. **5**, 23 (1958).
[3] K. Okamoto, Phys. Rev. **110**, 143 (1958).
[4] T. Kishimoto, J. M. Moss, D. H. Youngblood, J. D. Bronson, C. M. Rozsa, D. R. Brown, and A. D. Bacher, Phys. Rev. Lett. **35**, 552 (1975).
[5] T. Nakatsukasa, K. Matsuyanagi, and S. Mizutori, Prog. Theor. Phys. **87**, 607 (1992).
[6] R. Nazmitdinov and S. Åberg, Phys. Lett. B **289**, 238 (1992).
[7] T. Suzuki and D. J. Rowe, Nucl. Phys. **A289**, 461 (1978).
[8] D. Zawischa, J. Speth, and D. Pal, Nucl. Phys. **A311**, 445 (1978).
[9] S. Aberg, Nucl. Phys. **A473**, 1 (1987).
[10] N. Lo Iudice and F. Palumbo, Phys. Rev. Lett. **41**, 1532 (1978).
[11] D. Bohle, A. Richter, W. Steffen, A. E. L. Dieperink, N. Lo Iudice, F. Palumbo, and O. Scholten, Phys. Lett. **137B**, 27 (1984).
[12] For an exhaustive list of references see N. Lo Iudice, Riv. Nuovo Cimento **9**, 1 (2000).
[13] P. Ring and P. Schuck, *The Nuclear Many-Body Problem* (Springer-Verlag, New York, 1980).
[14] J. Kvasil and R. G. Nazmitdinov, Fiz. Elem. Chastits At. Yadra **17**, 613 (1986) [Sov. J. Part. Nucl. **17**, 265 (1986)].
[15] Y. R. Shimizu and M. Matsuzaki, Nucl. Phys. **A558**, 559 (1995).
[16] L. M. Robledo, J. L. Egido, and P. Ring, Nucl. Phys. **A449**, 201 (1986).
[17] R. G. Nazmitdinov, Yad. Fiz. **46**, 732 (1987) [Sov. J. Nucl. Phys. **46**, 412 (1987)].
[18] T. Nakatsukasa, K. Matsuyanagi, S. Mizutori, and Y. R. Shimizu, Phys. Rev. C **53**, 2213 (1996).
[19] Y. R. Shimizu, J. D. Garrett, R. A. Broglia, M. Gallardo, and E. Vigezzi, Rev. Mod. Phys. **61**, 131 (1989).
[20] D. Almehed, D. F. Dönau, S. Frauendorf, and R. G. Nazmitdinov, Phys. Scr. **T88**, 62 (2000); D. Almehed, S. Frauendorf, and F. Dönau, Phys. Rev. C **63**, 044311 (2001).
[21] K. A. Snover, Annu. Rev. Nucl. Part. Sci. **36**, 545 (1986) and references therein.
[22] J. J. Gaardhøje, Annu. Rev. Nucl. Part. Sci. **42**, 483 (1992) and references therein.
[23] Y. R. Shimizu and K. Matsuyanagi, Prog. Theor. Phys. **72**, 1017 (1984); **75**, 1167 (1986).
[24] See, for instance, J. Kvasil and R. G. Nazmitdinov, Phys. Rev. C **69**, 031304 (2004); J. Kvasil, R. G. Nazmitdinov, and A. S. Sitdikov, Yad. Fiz. (to be published).
[25] C. De Coster and K. Heyde, Phys. Rev. Lett. **63**, 2797 (1989).
[26] C. De Coster and K. Heyde, Nucl. Phys. **A524**, 441 (1991).
[27] J. Kvasil, N. Lo Iudice, V. O. Nesterenko, and M. Kopal, Phys. Rev. C **58**, 209 (1998).
[28] H. Sakamoto and T. Kishimoto, Nucl. Phys. **A501**, 205 (1989).
[29] N. Lo Iudice, Nucl. Phys. **A605**, 61 (1996).
[30] D. Almehed, F. Dönau, and R. G. Nazmitdinov, J. Phys. G **29**, 2193 (2003).
[31] R. G. Nazmitdinov, D. Almehed, and F. Dönau, Phys. Rev. C **65**, 041307(R) (2002).
[32] E. R. Marshalek, Nucl. Phys. **A266**, 317 (1976).
[33] A. K. Jain, R. K. Sheline, P. C. Sood, and K. Jain, Rev. Mod. Phys. **62**, 393 (1990).
[34] R. Wyss, W. Satula, W. Nazarewicz, and A. Johnson, Nucl. Phys. **A511**, 324 (1990).
[35] R. Ch. Safarov and A. S. Sitdikov, Izv. Akad. Nauk, Ser. Fiz. **63**, 162 (1999) and references therein.
[36] S. Frauendorf and F. R. May, Phys. Lett. **125B**, 245 (1983).
[37] B. Castel and I. Hamamoto, Phys. Lett. **65B**, 27 (1976).
[38] N. Lo Iudice and A. Richter, Phys. Lett. B **228**, 291 (1989).
[39] A. Richter, Nucl. Phys. **A553**, 417c (1993).
[40] F. Palumbo and A. Richter, Phys. Lett. **158B**, 101 (1985).
[41] N. Lo Iudice, E. Lipparini, S. Stringari, F. Palumbo, and A. Richter, Phys. Lett. **161B**, 18 (1985).
[42] L. Zamick and D. C. Zheng, Phys. Rev. C **44**, 2522 (1991).
[43] N. Lo Iudice, Phys. Rev. C **57**, 1246 (1998).
[44] N. Lo Iudice and A. Richter, Phys. Lett. B **304**, 193 (1993).
[45] N. Pietralla, P. von Brentano, R.-D. Herzberg, U. Kneissl, N. Lo Iudice, H. Maser, H. H. Pitz, and A. Zilges, Phys. Rev. C **58**, 184 (1998).
[46] W. Ziegler, C. Rangacharyulu, A. Richter, and C. Spieler, Phys. Rev. Lett. **65**, 2515 (1990).
[47] J. Margraf, R. D. Heil, U. Kneissl, U. Meier, H. H. Pitz, H. Friedrichs, S. Lindenstruth, B. Schlitt, C. Wesselborg, P. von Brentano, R.-D. Herzberg, and A. Zilges, Phys. Rev. C **47**, 1474 (1993).